TOPOLOGICAL DERIVATIVES OF SHAPE FUNCTIONALS. PART 3
SECOND ORDER METHOD AND APPLICATIONS

A.A. NOVOTNY, J. SOKOŁOWSKI, AND A. ŻOCHOWSKI

Abstract. The framework of asymptotic analysis in singularly perturbed geometrical domains presented in the first part of this series of review papers can be employed in order to produce the two terms asymptotic expansions for a class of shape functionals. In the second part of review the one term expansions of functional are required for the algorithm of shape-topological optimization. Such an approach corresponds to the simple gradient method in shape optimization. The Newton method of shape optimization can be replaced for the shape-topology optimization by the two terms expansions of shape functionals. Thus, the obtained approximations are more precise and the associated numerical method is much more performed and complex compared to the one term expansion topological derivative algorithm. In particular, the numerical algorithm associated with the first order topological derivative of shape functionals has been presented in the second part the review, together with an account on its applications currently found in the literature, with emphasis on shape and topology optimization. In this third and last part the second order topological derivative is introduced. The second order algorithm of shape-topological optimization is used for numerical solution of representative examples for inverse reconstruction problems. The main feature of the shape-topology optimization algorithm is the property that the method is non-iterative and thus very robust with respect to noisy data as well as free of initial guess.

1. Introduction

The topological sensitivity analysis, presented in the first part of this series of review papers, leads to the asymptotic expansion of a given shape functional with respect to a small parameter that measures the size of singular domain perturbations, such as holes, inclusions, source-terms and cracks. This relatively new concept has applications in many different fields such as shape and topology optimization, inverse problems, imaging processing, multi-scale material design and mechanical modeling including damage and fracture evolution phenomena. The numerical algorithm associated with the first order topological derivative has been presented in the second part of this series of review papers, together with an account on its applications currently found in the literature, with emphasis on shape and topology optimization.

In this third and last part of review papers, the concept of second order topological derivative is introduced [20], which are used for solving a class of inverse reconstruction problems written in the form of overdetermined boundary value problems. The general idea consists in rewrite then as a topology optimization problem. In particular, a shape functional measuring the misfit between the boundary measurements and the solution obtained from the model is minimized with respect to a set of ball-shaped anomalies by using the concept of topological derivatives. It means that the objective functional is expanded and then truncated up to the second order term, leading to a quadratic and strictly convex form with respect to the parameters under consideration. Thus, a trivial optimization step leads to a non-iterative second order reconstruction algorithm. As a result, the reconstruction process becomes very robust with respect to noisy data and independent of any initial guess. Finally, these results are used for solving a wide class of inverse reconstruction problems.

The paper is organized as following. The second order topological derivative concept is introduced in Section 2. The resulting second order method is presented in Section 3, together with the associated algorithm. In Section 4 a class of inverse reconstruction problems written in the form of overdetermined boundary value problems is introduced. In particular, Section 4.1

Key words and phrases. Topological derivatives, second order method, applications in inverse problems.

deals with the inverse conductivity problem. The inverse gravimetry problem is presented in Section 4.2. A pointwise source reconstruction problem is introduced in Section 4.3. Section 4.4 is dedicated to an obstacle reconstruction problem. In Section 4.5 the inverse electromagnetic casting problem is discussed. Finally, the paper ends with some concluding remarks and open problems in Section 5.

2. Preliminaries

Let us consider an open and bounded domain $\Omega \subset \mathbb{R}^d$, $d \geq 2$, with Lipschitz continuous boundary $\partial\Omega$. The domain Ω is subjected to a perturbation confined in a small arbitrary-shaped set $\omega_\varepsilon(\widehat{x})$ of size ε and center at an arbitrary point $\widehat{x}$ of Ω, such that $\overline{\omega_\varepsilon(\widehat{x})} \subset \Omega$. We introduce a characteristic function $x \mapsto \chi(x)$, $x \in \Omega$, associated to the unperturbed domain, namely $\chi = \mathbb{1}_\Omega$. Then, we define a characteristic function associated to the topologically perturbed domain of the form $x \mapsto \chi_\varepsilon(\widehat{x}; x)$, $x \in \Omega$. In the case of a hole, for example, $\chi_\varepsilon(\widehat{x}) = \mathbb{1}_\Omega - \mathbb{1}_{\overline{\omega_\varepsilon(\widehat{x})}}$ and the perturbed domain is given by $\Omega_\varepsilon(\widehat{x}) = \Omega \setminus \overline{\omega_\varepsilon(\widehat{x})}$. Then, we assume that a given shape functional $\psi(\chi_\varepsilon(\widehat{x}))$, associated to the topologically perturbed domain, admits the following topological asymptotic expansion [35]

$$\psi(\chi_\varepsilon(\widehat{x})) = \psi(\chi) + f_1(\varepsilon)\mathcal{T}(\widehat{x}) + f_2(\varepsilon)\mathcal{T}^2(\widehat{x}) + o(f_2(\varepsilon)) \,, \tag{2.1}$$

where $\psi(\chi)$ is the shape functional associated to the unperturbed domain, $f_1(\varepsilon)$ and $f_2(\varepsilon)$ are positive functions and $o(f_2(\varepsilon))$ is the remainder, such that $f_1(\varepsilon) \to 0$, $f_2(\varepsilon)/f_1(\varepsilon) \to 0$ and $o(f_2(\varepsilon))/f_2(\varepsilon) \to 0$ when $\varepsilon \to 0$, respectively. The functions $\widehat{x} \mapsto \mathcal{T}(\widehat{x})$ and $\widehat{x} \mapsto \mathcal{T}^2(\widehat{x})$ are called first and second order topological derivatives of ψ at $\widehat{x}$. The terms $f_1(\varepsilon)\mathcal{T}(\widehat{x})$ and $f_2(\varepsilon)\mathcal{T}^2(\widehat{x})$ represent, respectively, first and second order corrections of $\psi(\chi)$ to approximate $\psi(\chi_\varepsilon(\widehat{x}))$. Therefore, the first order topological derivative $\mathcal{T}(\widehat{x})$ can naturally be used as a steepest-descent direction in an optimization process like in any method based on the gradient of the cost functional, leading to a family of first order topology optimization algorithms. On the other hand, the second order topological derivative $\mathcal{T}^2(\widehat{x})$ leads to second order topology optimization algorithms, which are non-iterative and thus very robust with respect to noisy data, for instance. Since all quantities on the right-hand side of (2.1) are defined in the original (unperturbed) domain Ω, the resulting algorithms derived from $\mathcal{T}(\widehat{x})$ and $\mathcal{T}^2(\widehat{x})$ are free of initial guess.

The form of the topological asymptotic expansion (2.1) depends on many features of the problem under consideration, including the spatial dimension, differential operator, nature of the topological perturbations and their boundary/transmission conditions, etc. In order to fix these ideas, let us consider the elasticity problem into tree spatial dimensions, whose topological perturbation is given by the nucleation of an arbitrary shaped inclusion endowed with different material properties from the background. According to [7], in this case expansion (2.1) takes the form

$$\psi(\chi_\varepsilon(\widehat{x})) = \psi(\chi) + \varepsilon^3\mathcal{T}(\widehat{x}) + \varepsilon^4\mathcal{T}^2(\widehat{x}) + \varepsilon^5\mathcal{T}^3(\widehat{x}) + \varepsilon^6\mathcal{T}^4(\widehat{x}) + o(\varepsilon^6) \,. \tag{2.2}$$

For spherical or ellipsoidal shaped inclusions, the $O(\varepsilon^4)$ term vanishes. See also [25] for equivalent expansion in the scalar case. Into two spatial dimensions the topological asymptotic analysis may becomes more involved. In fact, depending on the problem under consideration, logarithm of ε may appear. See for instance Section 4.4. Let us remark however that this is a rich and fascinating field of research with a wide range of relevant applications and many unsolved theoretical questions. See Section 5 for an account on some open problems.

3. Second Order Algorithm

A well known phenomenon concerning high order topological asymptotic expansion concerns the interaction between several topological perturbations. Therefore, let us consider that the domain Ω is perturbed by the nucleation of N ball-shaped anomalies $B_{\varepsilon_i}(x_i)$ of radii ε_i and centers at $x_i \in \Omega$, with $i = 1, \cdots, N$. We introduce the notations $\xi = (x_1, \cdots, x_N)$ and

$\varepsilon = (\varepsilon_1, \cdots, \varepsilon_N)$. We restrict ourselves to the case in which expansion (2.1) takes the following quadratic form with respect to α

$$\psi(\chi_\varepsilon(\xi)) = \psi(\chi) - \alpha \cdot d(\xi) + \frac{1}{2} H(\xi)\alpha \cdot \alpha + \mathcal{E}(\varepsilon) \ , \tag{3.1}$$

where $\alpha = (\alpha_1, ..., \alpha_N)$, with $\alpha_i = f_1(\varepsilon_i)$, and $\mathcal{E}(\varepsilon)$ is the remainder. The vector $d \in \mathbb{R}^N$ and the Hessian matrix $H \in \mathbb{R}^N \times \mathbb{R}^N$ represent the fist and second order topological derivatives, respectively. Theirs entries are defined as d_i and H_{ij}. In addition, the expression on the right-hand side of (3.1) shall depends on the number N of anomalies, their sizes α and locations ξ. Thus, from (3.1), we can define the following quantity:

$$\delta J(\alpha, \xi, N) := -\alpha \cdot d(\xi) + \frac{1}{2} H(\xi)\alpha \cdot \alpha \ , \tag{3.2}$$

Let us assume that the infinity dimensional Hessian matrix $H(\xi)$ is positive definite, so that the minimization of the function $\delta J(\alpha, \xi, N)$ with respect to the variable α yields

$$\langle D_\alpha \delta J, \beta \rangle = (H(\xi)\alpha - d(\xi)) \cdot \beta = 0, \quad \forall \beta \ , \tag{3.3}$$

which leads to the following linear system

$$H(\xi)\alpha = d(\xi) \ . \tag{3.4}$$

The quantity α solution of (3.4) becomes a function of the locations ξ, namely $\alpha = \alpha(\xi)$. Let us now replace the solution of (3.4) into $\delta J(\alpha, \xi, N)$ defined by (3.2). Therefore, the optimal locations $\xi^\star$ can be trivially obtained from a combinatorial search over the domain Ω, solution to the following minimization problem

$$\xi^\star = \underset{\xi \in X}{\operatorname{argmin}} \left\{ \delta J(\alpha(\xi), \xi, N) = -\frac{1}{2} \alpha(\xi) \cdot d(\xi) \right\} \ , \tag{3.5}$$

where X is the set of admissible anomalies locations. Finally, the optimal intensities are given by $\alpha^\star = \alpha(\xi^\star)$. In summary, our method is able to find optimal sizes $\alpha^\star$ of the hidden anomalies and theirs locations $\xi^\star$ for a given number N of trials balls.

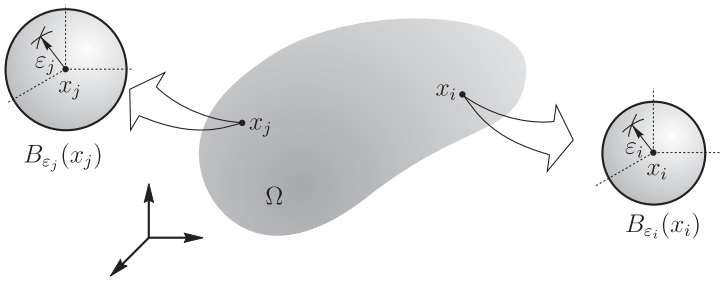

FIGURE 1. Nucleation of a set of ball-shaped inclusions $B_{\varepsilon_i}(x_i)$, $i = 1, \cdots, N$.

In order to summarize the calculations presented in this section we introduce now the resulting second order topology optimization algorithm. It describes the process of obtaining the optimal parameters $\alpha^\star$ and $\xi^\star$ from the computational point of view. The entries of the algorithm are listed below:

- The quantity N of anomalies;
- The M-points on which the systems (3.4) are solved;
- The vector d and the matrix H, whose entries are given by $f(i) := d_i$ and $A(i, j) := H_{ij}$, respectively.

The algorithm returns optimal sizes $\alpha^\star$ and locations $\xi^\star$. The above procedure written in pseudo-code format is shown in Algorithm 1. In the algorithm, Π maps the vector of nodal indices $\mathcal{I} = (i_1, i_2, ..., i_N)$ into the corresponding vector of nodal coordinates ξ. For further applications of this algorithm we refer to [11, 12, 21, 33, 36], for instance.

Algorithm 1: Second Order Algorithm.

input : d, H, M, N;
output: the optimal solution $S^\star$, $\alpha^\star$, $\xi^\star$;

Initialization: $S^\star \leftarrow \infty$; $\alpha^\star \leftarrow 0$; $\xi^\star \leftarrow 0$;
for $i_1 \leftarrow 1$ **to** M **do**
  for $i_2 \leftarrow i_1 + 1$ **to** M **do**
    $\vdots$
    for $i_N \leftarrow i_{N-1} + 1$ **to** M **do**

$$d \leftarrow \begin{bmatrix} f(i_1) \\ f(i_2) \\ \vdots \\ f(i_N) \end{bmatrix}; \quad H \leftarrow \begin{bmatrix} A(i_1,i_1) & A(i_1,i_2) & \cdots & A(i_1,i_N) \\ A(i_2,i_1) & A(i_2,i_2) & \cdots & A(i_2,i_N) \\ \vdots & \vdots & \ddots & \vdots \\ A(i_N,i_1) & A(i_N,i_2) & \cdots & A(i_N,i_N) \end{bmatrix};$$

      $\mathcal{I} \leftarrow (i_1, i_2, ..., i_N)$; $\xi \leftarrow \Pi(\mathcal{I})$; $\alpha \leftarrow H^{-1}d$; $S \leftarrow -\frac{1}{2} d \cdot \alpha$;
      if $S < S^\star$ **then**
        $\xi^\star \leftarrow \xi$; $\alpha^\star \leftarrow \alpha$; $S^\star \leftarrow S$;
      end if
    end for
  end for
end for
return $S^\star$, $\alpha^\star$, $\xi^\star$;

As can be noted in the Algorithm 1, the optimal solution $(\xi^\star, \alpha^\star)$ is obtained through an combinatorial and exhaustive search over the M-points. Therefore, the complexity $\mathcal{C}(M,N)$ of the algorithm can be evaluated by the formula:

$$\mathcal{C}(M,N) = \left(\begin{array}{c} M \\ N \end{array} \right) N^3 = \frac{M!}{N!(M-N)!} N^3. \tag{3.6}$$

In Fig. 2 the graphics of $N \times \log_{10}(\mathcal{C}(M,N))$ for $M = 100$ and $M = 400$ are presented in blue and red, respectively.

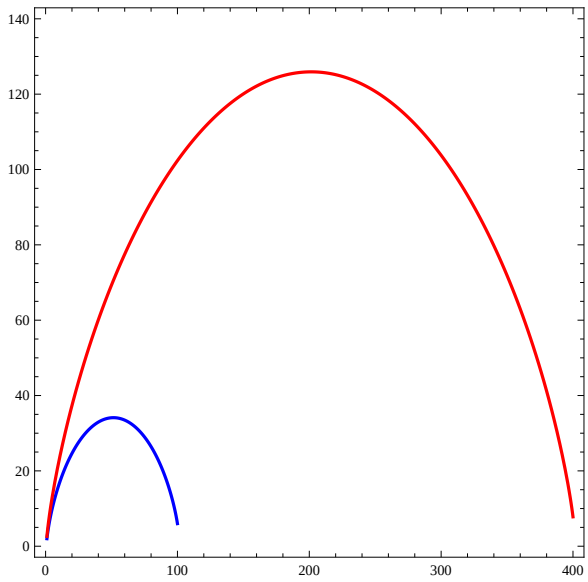

FIGURE 2. Complexity order of Algorithm 1: $N \times \log_{10}(\mathcal{C}(M,N))$, for $M = 100$ in blue and $M = 400$ in red.

Since Algorithm 1 is the bottleneck of the proposed second order topology optimization method, we refer to [33] for more sophisticated approaches based on meta-heuristic and multi-grid versions of Algorithm 1. In addition, the approximation of the solution by a finite number of balls can be seen as a limitation of our approach. However, the reconstruction obtained may serve as an initial guess for other well-established and more computationally sophisticated iterative methods [9, 24, 28, 32, 38].

4. Inverse Reconstruction Problems

In this section the topological derivative concept is applied in the context of a class of inverse problems in imaging. A wide class of inverse problems can be written in the form of overdetermined boundary value problems. Such a difficult can be overcome by rewriting the inverse problem in the form of an optimization problem. The basic idea consists in minimize an objective functional measuring the misfit between a given data and a numerical solution with respect to the parameters under consideration. In particular, let us consider a geometrical domain Ω with its boundary denoted as $\Gamma = \partial\Omega$. A boundary value problem is defined in Ω, whose solution is denoted by u^*. We assume that the response of the system on the boundary Γ can be observed. For example, given a Dirichlet data U on Γ, the associated Dirichlet-to-Neumann map for a second order elliptic equation is defined as follows [10]

$$\Lambda_{\omega^*} \ : \ u^* = U \mapsto Q := \partial_n u^* \quad \text{on} \quad \Gamma.$$

where ω^* is an unknown set of anomalies embedded within Ω and n is the exterior unit normal vector on Γ. Therefore, given the pair (U, Q) we want to reconstruct the set $\omega^* \subset \Omega$. The mathematical model of the system furnishes the mapping $\omega \mapsto \Lambda_\omega$ for a family of anomalies ω. Thus, taking U we can generate the output of the model $\Lambda_\omega(U)$ and compare it with the given function $Q = \Lambda_{\omega^*}(U)$. Hence, using the mathematical model we can consider the associated optimization problem based on the distance minimization between the observation (U, Q) and the model response $(U, \Lambda_\omega(U))$ over the family of admissible anomalies ω. This is a numerical method which uses the shape and topological derivatives of the specific shape functional defined for the inverse problem [5, 11, 17, 18, 23, 24, 25, 29, 31, 34]. In particular, we are going to apply the second order topology design Algorithm 1 for solving a class of inverse reconstruction problem. See also related works [3, 8, 15, 16, 19, 22].

4.1. Inverse Conductivity Problem.

The electrical impedance tomography (EIT) problem consists in determining the distribution of the electrical conductivity of a medium subject to a set of current fluxes, from measurements of the corresponding electrical potentials on its boundary. EIT is probably the most studied inverse problem since the fundamental works by Calderón from the eighties [10]. It has many relevant applications in medicine (detection of tumors), geophysics (localization of mineral deposits) and engineering (detection of corrosion in structures). Following the original ideas presented in [21], we are interested in reconstructing a number of anomalies with different electrical conductivity from the background. In particular, a shape functional measuring the misfit between the boundary measurements and the electrical potentials obtained from the model is minimized with respect to a set of ball-shaped anomalies by using the concept of topological derivatives. Let us consider a domain $\Omega \subset \mathbb{R}^2$ with Lipschitz continuous boundary $\partial\Omega$, which represents a body endowed with the capability of conducting electricity. Its electrical conductivity coefficient is denoted by $k^*(x) \geq k_0 > 0$, with $x \in \Omega$ and $k_0 \in \mathbb{R}_+$. If the body Ω is subjected to a given electric flux Q on $\partial\Omega$, then the resulting electric potential in Ω is observed on a part of the boundary $\Gamma_M \subset \partial\Omega$. The objective is to reconstruct the electrical conductivity k^* over Ω from the obtained partial boundary measurement $U := u^*_{|\Gamma_M}$, solution of the following over-determined boundary value problem

$$\left\{ \begin{array}{rcll} \operatorname{div}[q(u^*)] & = & 0 & \text{in } \Omega, \\ q(u^*) & = & -k^* \nabla u^*, & \\ q(u^*) \cdot n & = & Q & \text{on } \partial\Omega, \\ u^* & = & U & \text{on } \Gamma_M. \end{array} \right. \tag{4.1}$$

Without loss of generality, we are considering only one boundary measurement U on Γ_M. The extension to several boundary measurements is trivial. Furthermore, we assume that the unknown electrical conductivity k^* we are looking for belongs to the following set

$$C_\gamma(\Omega) := \left\{ \varphi \in L^\infty(\Omega) : \varphi = k \left(\mathbb{1}_\Omega - \sum_{i=1}^{N} (1-\gamma_i) \mathbb{1}_{\omega_i} \right) \right\}, \tag{4.2}$$

where $k \in \mathbb{R}_+$ is the electrical conductivity of the background. The sets $\omega_i \subset \Omega$, with $i = 1, \cdots, N$, are such that $\omega_i \cap \omega_j = \varnothing$, for $i \neq j$. In addition, $\mathbb{1}_\Omega$ and $\mathbb{1}_{\omega_i}$ are used to denote the characteristics functions of Ω and ω_i, respectively. Finally, $\gamma_i \in \mathbb{R}_+$ are the contrasts with respect to the electrical conductivity of the background k. See sketch in Fig. 3.

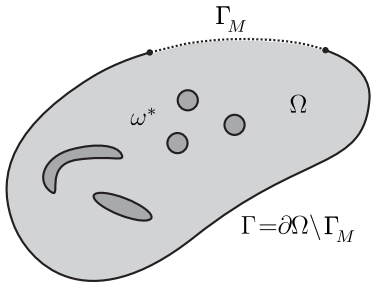

FIGURE 3. The Electrical Impedance Tomography problem.

We assume that the electrical conductivity of the background k and the associated contrasts γ_i are known. Therefore, the inverse problem we are dealing with can be written in the form of a topology optimization problem with respect to the sets $\omega = \bigcup_{i=1}^{N} \omega_i$. Let us introduce the following auxiliary Neumann boundary value problem: Find u, such that

$$\left\{ \begin{array}{rcll} \operatorname{div}[q(u)] & = & 0 & \text{in } \Omega \\ q(u) & = & -k_\omega \nabla u & \\ q(u) \cdot n & = & Q & \text{on } \partial\Omega \\ \int_{\partial\Omega} Q & = & 0 & \\ \int_{\Gamma_M} u & = & \int_{\Gamma_M} U, & \end{array} \right. \tag{4.3}$$

where $Q \in H^{-1/2}(\partial\Omega)$ and $U \in H^{1/2}(\Gamma_M)$ are the boundary excitation and boundary measurement, respectively, and $k_\omega \in C_\gamma(\Omega)$ is constant by parts, characterized by a set $\omega \subset \Omega$. Finally, we introduce the following shape functional measuring the misfit between the boundary measurement U and the solution $u = u(\omega)$ of (4.3) evaluated on Γ_M, namely

$$\underset{\omega \subset \Omega}{\text{Minimize}}\ \mathcal{J}_\omega(u) = \int_{\Gamma_M} (u(\omega) - U)^2, \tag{4.4}$$

which will be solved by using the first and second order topological derivatives concepts. See related works [1, 2, 4, 6, 25, 37].

We consider $\omega = \varnothing$ as initial guess, so that $k_{\omega|_{\omega=\varnothing}} = k$ in (4.3). The domain Ω is perturbed by the nucleation of N ball-shaped inclusions of radii ε_i and centers at $x_i \in \Omega$, endowed with contrasts γ_i, $i = 1, \cdots, N$. From these elements, $\alpha = (\varepsilon_1^2, \cdots, \varepsilon_N^2)$ and $\mathcal{E}(\varepsilon) = o(|\alpha|^2)$ in (3.1). In addition, the entries of the vector $d(\xi) \in \mathbb{R}^N$ is defined as

$$d_i = 2 \int_{\Gamma_M} \rho_i (u - U)(g_i + \tilde{u}_i), \tag{4.5}$$

while the entries of the matrix $H(\xi) \in \mathbb{R}^N \times \mathbb{R}^N$ is given by

$$H_{ii} = 4 \int_{\Gamma_M} (u - U)(\rho_i h_i + \rho_i \tilde{g}_i + \tilde{\tilde{u}}_i) + 2 \int_{\Gamma_M} (\rho_i g_i + \tilde{u}_i)^2, \tag{4.6}$$

$$H_{ij} = 2\int_{\Gamma_M} (u-U)(\rho_j\theta_i^j + \rho_i\theta_j^i + u_i^j + u_j^i) \\ + 2\int_{\Gamma_M} (\rho_i g_i + \tilde{u}_i)(\rho_j g_j + \tilde{u}_j), \qquad j \neq i. \quad (4.7)$$

Some terms in the above equations still requires explanation. The coefficient ρ_i is defined as

$$\rho_i = \frac{1-\gamma_i}{1+\gamma_i}, \quad (4.8)$$

and the functions $g_i(x)$, $h_i(x)$, $\tilde{g}_i(x)$ and $\theta_i^j(x)$ are respectively given by

$$g_i(x) = \frac{1}{\|x-x_i\|^2}\nabla u(x_i)\cdot(x-x_i), \quad (4.9)$$

$$h_i(x) = \frac{1}{2}\frac{1}{\|x-x_i\|^4}\nabla^2 u(x_i)(x-x_i)^2, \quad (4.10)$$

$$\tilde{g}_i(x) = \frac{1}{\|x-x_i\|^2}\nabla \tilde{u}_i(x_i)\cdot(x-x_i), \quad (4.11)$$

$$\theta_i^j(x) = \frac{1}{\|x-x_j\|^2}A(x_j)\nabla u(x_i)\cdot(x-x_j). \quad (4.12)$$

where the second order tensor $A(x)$ is written as

$$A(x) = \frac{1}{\|x-x_i\|^2}\left[I - 2\frac{(x-x_i)\otimes(x-x_i)}{\|x-x_i\|^2}\right]. \quad (4.13)$$

Finally, the auxiliary function $\tilde{u}_i$ is solution to: Find $\tilde{u}_i$, such that

$$\begin{cases} \operatorname{div}[q(\tilde{u}_i)] = 0, & \text{in } \Omega, \\ q(\tilde{u}_i) = -k\nabla\tilde{u}_i, & \text{in } \Omega, \\ q(\tilde{u}_i)\cdot n = -\rho_i q(g_i)\cdot n, & \text{on } \partial\Omega \\ \int_{\Gamma_M}\tilde{u}_i = -\rho_i\int_{\Gamma_M} g_i, \end{cases} \quad (4.14)$$

while the auxiliary function $\tilde{\tilde{u}}_i$ solves: Find $\tilde{\tilde{u}}_i$, such that

$$\begin{cases} \operatorname{div}[q(\tilde{\tilde{u}}_i)] = 0 & \text{in } \Omega, \\ q(\tilde{\tilde{u}}_i) = -k\nabla\tilde{\tilde{u}}_i & \text{in } \Omega, \\ q(\tilde{\tilde{u}}_i)\cdot n = -\rho_i q(h_i+\tilde{g}_i)\cdot n, & \text{on } \partial\Omega \\ \int_{\Gamma_M}\tilde{\tilde{u}}_i = -\rho_i\int_{\Gamma_M} h_i + \tilde{g}_i, \end{cases} \quad (4.15)$$

and the auxiliary function u_i^j is solution to: Find u_i^j, such that

$$\begin{cases} \operatorname{div}[q(u_i^j)] = 0 & \text{in } \Omega, \\ q(u_i^j) = -k\nabla u_i^j & \text{in } \Omega, \\ q(u_i^j)\cdot n = -\rho_j q(\theta_i^j)\cdot n, & \text{on } \partial\Omega \\ \int_{\Gamma_M} u_i^j = -\rho_j\int_{\Gamma_M}\theta_i^j. \end{cases} \quad (4.16)$$

The derivation of the above equations can be found in [21], for instance.

Now, we have all elements to apply Algorithm 1 for solving the proposed conductivity reconstruction problem (4.4). In fact, let us present a numerical example. We consider a disk of unit radius. Its boundary is subdivided into 16 disjoint pieces. Each pair of such a pieces is used for injecting and draining the current. Therefore, the excitation Q is given by a pair $Q_{\text{in}} = 1$ of injection and $Q_{\text{out}} = -1$ of draining. The remainder part of the boundary remains insulated. The associated potential U is measured only on these disjoint pieces, representing Γ_M. The target consists of three ball-shaped anomalies, which is corrupted with 10% of White Gaussian Noise, as shown in Fig. 4(a). The obtained reconstruction with 64 partial boundary measurements is shown in Fig. 4(b).

From an inspection of Fig. 3 we observe that the proposed method is actually very robust with respect to noisy data. It comes out from the fact that the devised second-order reconstruction algorithm is non-iterative.

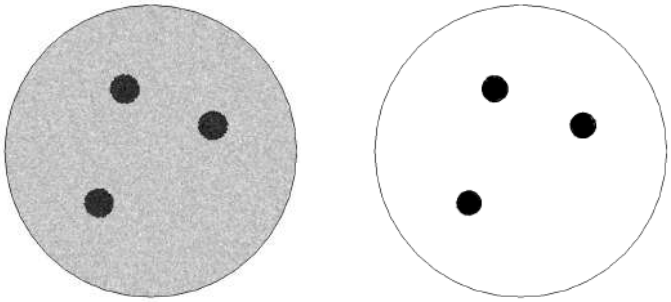

(a) target (b) result

FIGURE 4. Target corrupted with 10% of White Gaussian Noise and obtained result with 64 partial boundary measurements for the EIT problem [21].

4.2. **Inverse Gravimetry Problem.** The inverse gravimetry problem consists in reconstructing the mass distribution in a geometrical domain, from measurements of the gravity force on its boundary [27]. Based on [12], the inverse problem is reformulated as a topology optimization problem, where the support of the mass distribution is the unknown variable. The Kohn–Vogelius functional, which measures the misfit between the solutions of two auxiliary problems, one containing information about the boundary measurement and the other one containing information on the boundary excitation, is minimized. The Newtonian potential is used to complement the unavailable information about the hidden boundary. The resulting topology optimization algorithm is based on an analytic formula for the variation of the Kohn–Vogelius functional with respect to a class of mass distributions consisting of a finite number of ball-shaped trial anomalies.

In particular, let us consider an open and bounded domain $\Omega \subset \mathbb{R}^3$, with Lipschitz boundary $\partial\Omega$. We introduce the boundary $\Gamma_M \subset \partial\Omega$ where the measurements are taken and $\Gamma = \partial\Omega \setminus \Gamma_M$ the remainder (hidden) boundary, where there is no any information. We assume that the unknown density of the medium b^* belongs to the following set of admissible sources

$$C_\gamma(\Omega) := \left\{ \varphi \in L^\infty(\Omega) : \varphi = \sum_{i=1}^{N} \gamma_i \mathbb{1}_{\omega_i} \right\}, \tag{4.17}$$

where the sets $\omega_i \subset \Omega$, with $i = 1, \cdots, N$, are such that $\omega_i \cap \omega_j = \varnothing$, for $i \neq j$. In addition, $\mathbb{1}_{\omega_i}$ is used to denote the characteristic function of ω_i. Finally, $\gamma_i \in \mathbb{R}_+$ are the contrasts with respect to the density of the background, which are assumed to be known. From $b^* \in C_\gamma(\Omega)$ we define the associated potential as [28]

$$u(x) = \int_\Omega K(x,y) b^*(y)\, dy \,, \tag{4.18}$$

where the kernel $K(x,y)$ is given by

$$K(x,y) = \frac{1}{4\pi\|x-y\|}. \tag{4.19}$$

The pair of boundary measurements (U, Q) are defined as

$$U := u_{|\Gamma_M} \quad \text{and} \quad Q := -\partial_n u_{|\Gamma_M} \,, \tag{4.20}$$

where n is the outward unit normal vector to Ω.

Therefore, the inverse gravimetry problem we are dealing with reads: given $Q \in H^{-1/2}(\Gamma_M)$ and $U \in H^{1/2}(\Gamma_M)$, find the unknown source $b^* \in C_\gamma(\Omega)$ such that there exists $u^* \in H^1(\Omega)$ satisfying the following overdetermined boundary value problem:

$$\left\{ \begin{array}{rcl} -\Delta u^* & = & b^* \\ u^* & = & U \\ -\partial_n u^* & = & Q \end{array} \right\} \begin{array}{l} \text{in} \quad \Omega \,, \\ \\ \text{on} \quad \Gamma_M \,, \end{array} \tag{4.21}$$

The inverse problem (4.21) is clearly ill-posed [26]. However, since the contrasts γ_i, $i = 1, \cdots N$, in (4.17) are assumed to be known, problem (4.21) can be written in the form of a topology optimization problem with respect to the sets $\omega = \bigcup_{i=1}^{N} \omega_i$. Therefore, we introduce the following topology optimization problem based on the minimization of the Kohn-Vogelius criterion [30] with respect to the support ω:

$$\underset{\omega \subset \Omega}{\text{Minimize}}\ \mathcal{J}_\omega(u^D, u^N) = \int_\Omega (u^D(\omega) - u^N(\omega))^2, \tag{4.22}$$

which will be solved by using the first and second order topological derivatives concepts. The auxiliaries functions $u^D = u^D(\omega)$ and $u^N = u^N(\omega)$ are respectively solutions to the following boundary values problems

$$\left\{ \begin{array}{rcl} -\Delta u^D &=& b_\omega \quad \text{in} \quad \Omega\,, \\ u^D &=& U \quad \text{on} \quad \Gamma_M\,, \\ u^D &=& u^T \quad \text{on} \quad \Gamma\,, \end{array} \right. \quad \text{and} \quad \left\{ \begin{array}{rcl} -\Delta u^N &=& b_\omega \quad \text{in} \quad \Omega\,, \\ -\partial_n u^N &=& Q \quad \text{on} \quad \Gamma_M\,, \\ u^N &=& u^T \quad \text{on} \quad \Gamma\,. \end{array} \right. \tag{4.23}$$

where $b_\omega \in C_\gamma(\Omega)$ and the Newtonian potential

$$u^T(x) = \int_\Omega K(x,y) b_\omega(y)\, dy \tag{4.24}$$

is used to complement the information on the hidden boundary Γ, with the kernel $K(x,y)$ given by (4.19). Note that the domain Ω and the part Γ of its boundary $\partial\Omega$ do not represent physical quantities and are introduced to get a meaningful mathematical model. Actually, the inverse gravimetry problem may e.g. be defined in the whole half space $\mathbb{R}^2 \times (-\infty, 0)$, as represented in Fig. 5. The only constraint on Ω is that it has to be large enough to contain any possible anomaly, since (4.24) is correct only if this requirement is satisfied. In the following we assume that any possible anomaly is in Ω.

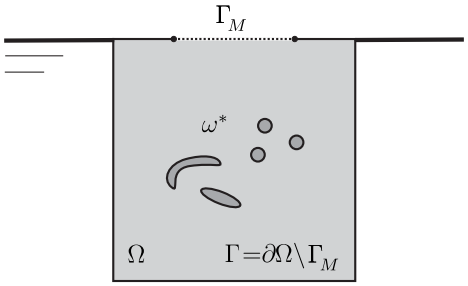

FIGURE 5. The inverse gravimetry problem.

We consider $\omega = \varnothing$ as initial guess, so that $b_{\omega|_{\omega=\varnothing}} = 0$. The domain Ω is perturbed by the nucleation of N ball-shaped anomalies of radii ε_i and centers at $x_i \in \Omega$, endowed with contrasts γ_i, $i = 1, \cdots, N$. From these elements, $\alpha = (|B_{\varepsilon_1}(x_1)|, \cdots, |B_{\varepsilon_N}(x_N)|)$ and $\mathcal{E}(\varepsilon) \equiv 0$ in (3.1), namely, there is no remainder in this case. In addition, the entries of vector $d(\xi) \in \mathbb{R}^N$ and matrix $H(\xi) \in \mathbb{R}^N \times \mathbb{R}^N$ are respectively defined as

$$d_i = 2\gamma_i \int_\Omega (u^D - u^N) h_i \quad \text{and} \quad H_{ij} = \gamma_i \gamma_j \int_\Omega h_i h_j\,. \tag{4.25}$$

Finally, the auxiliaries function $h_i(x)$ are solutions to the following boundary values problems depending on x_i

$$\left\{ \begin{array}{rcl} -\Delta h_i &=& 0 \quad \text{in} \quad \Omega\,, \\ -\partial_n h_i &=& g_i \quad \text{on} \quad \Gamma_M\,, \\ h_i &=& 0 \quad \text{on} \quad \Gamma\,, \end{array} \right. \tag{4.26}$$

where $g_i = \partial_n w_i$ on Γ_M with $w_i(x) = K(x, x_i) + v_i(x)$ and v_i solution to

$$\left\{ \begin{array}{rcll} -\Delta v_i & = & 0 & \text{in} \quad \Omega\,, \\ v_i & = & -K(x, x_i) & \text{on} \quad \Gamma_M\,, \\ v_i & = & 0 & \text{on} \quad \Gamma\,, \end{array} \right. \tag{4.27}$$

which is well defined provided that $x_i \notin \partial\Omega$. The derivation of the above equations follows the same steps as presented in [11], for instance. From the above elements, we are now in position to apply Algorithm 1 for solving the proposed source reconstruction problem (4.22).

Let us conclude this section with a numerical experiment in three spatial dimensions. In the example we take the cube $\Omega = (0,1) \times (0,1) \times (0,1)$. The partial boundary measurements are taken on the side of the cube $\Gamma_M = \{x = 1\} \cap \overline{\Omega}$. We are going to reconstruct three balls with centers $(0.7, 0.7, 0.4)$, $(0.6, 0.3, 0.3)$, $(0.5, 0.4, 0.8)$ and radii 0.17, 0.2, 0.15 respectively. The intensities $\gamma_i = 1$, for $i = 1, \cdots, 3$. We use synthetic measurements without noise in the data. Since in the set of ball-shaped anomalies there is no remainder in the expansion (3.1), we observe that Algorithm 1 reconstructs the positions and sizes of the three balls exactly. The result is shown in Fig. 6.

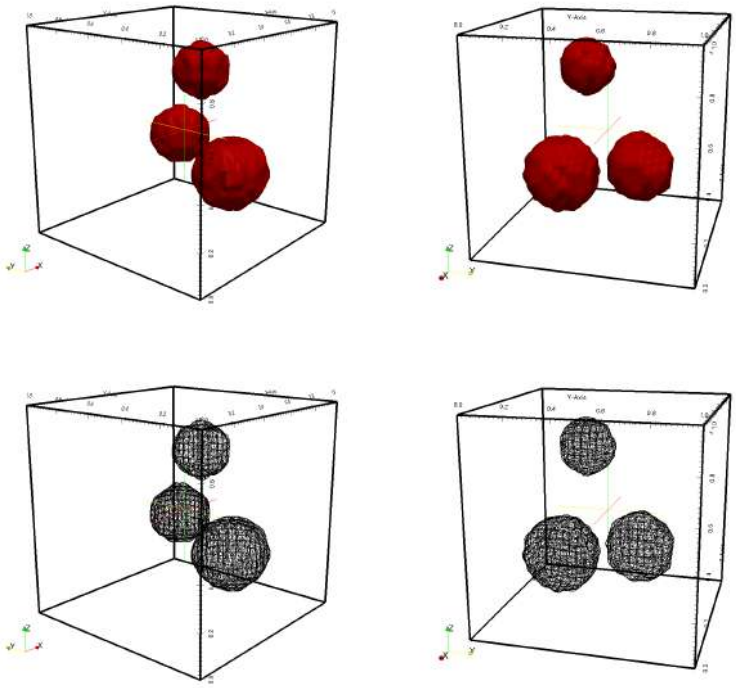

FIGURE 6. True anomalies (first row) and corresponding reconstructions (second row) for the gravimetry inverse problem [12].

4.3. **Pointwise Source Reconstruction Problem.** We consider a benchmark example concerning an inverse potential problem into two spatial dimensions. Let $\Omega \subset \mathbb{R}^2$ be an open and bounded domain with Lipschitz boundary $\partial\Omega$. The inverse problem we are dealing with consists in determining the unknown pointwise source $b^* \in C_\delta(\Omega)$ from the Cauchy data U and Q in the following elliptic boundary value problem:

$$\left\{ \begin{array}{rcll} -\Delta u^* & = & b^* & \text{in} \quad \Omega, \\ \left. \begin{array}{rcl} u^* & = & U \\ -\partial_n u^* & = & Q \end{array} \right\} & & & \text{on} \quad \partial\Omega. \end{array} \right. \tag{4.28}$$

where the set $C_\delta(\Omega)$ is defined as

$$C_\delta(\Omega) = \left\{ \varphi : \Omega \mapsto \mathbb{R} \mid \varphi(x) = \sum_{i=1}^{N} \alpha_i \delta(x - x_i) \right\}, \tag{4.29}$$

where $\alpha_i \in \mathbb{R} \setminus \{-\infty, +\infty\}$ and $x_i \in \Omega$, with $i = 1, \cdots, N$. Therefore, the unknown source $b^* \in C_\delta(\Omega)$ can be represented as follows:

$$b^*(x) = \sum_{i=1}^{N^*} \alpha_i^* \delta(x - x_i^*). \tag{4.30}$$

Thus, solving the above inverse potential problem in $C_\delta(\Omega)$ means to find N^*, α_i^* and x_i^*, which denote the number, intensities and locations of the unknown pointwise sources, respectively. Let us introduce the following functional based on the Kohn-Vogelius criterion [30]:

$$\underset{b \in C_\delta(\Omega)}{\text{Minimize}}\ \mathcal{J}(u^D, u^N) = \int_\Omega (u^D(\omega) - u^N(\omega))^2, \tag{4.31}$$

where the functions u^D and u^N are solutions to the following auxiliaries problems

$$\left\{ \begin{array}{rcl} -\Delta u^D &=& b \quad \text{in} \quad \Omega, \\ u^D &=& U \quad \text{on} \quad \partial\Omega. \end{array} \right. \quad \text{and} \quad \left\{ \begin{array}{rcl} -\Delta u^N &=& b + c \quad \text{in} \quad \Omega, \\ -\partial_n u^N &=& Q \quad \text{on} \quad \partial\Omega, \\ \int_\Omega u^N &=& \int_\Omega u^D, \end{array} \right. \tag{4.32}$$

where $b \in C_\delta(\Omega)$ is a given source, representing an initial guess. In addition, the compatibility constant c is given by

$$c = \frac{1}{|\Omega|} \left(\int_{\partial\Omega} Q - \int_\Omega b \right), \tag{4.33}$$

where $|\Omega|$ is the Lebesgue measure of the set Ω.

Let us now perturb the source b by introducing a number N of pointwise sources with arbitrary locations $x_i \in \Omega$ and intensities α_i, with $i = 1, \cdots, N$. The perturbed source $b_\delta \in C_\delta(\Omega)$ is defined as follows

$$b_\delta(x) = b(x) + \sum_{i=1}^{N} \alpha_i \delta(x - x_i). \tag{4.34}$$

For this class of perturbations, the vector $d(\xi) \in \mathbb{R}^N$ and matrix $H(\xi) \in \mathbb{R}^N \times \mathbb{R}^N$ in (3.4) can be obtained explicitly, whose entries are given by

$$d_i = \int_\Omega h_i (u^D - u^N) \quad \text{and} \quad H_{ij} = \int_\Omega h_i h_j, \tag{4.35}$$

where the auxiliaries function h_i are solutions to

$$\left\{ \begin{array}{rcl} -\Delta h_i &=& |\Omega|^{-1} \quad \text{in} \quad \Omega, \\ -\partial_n h_i &=& \partial_n v_i \quad \text{on} \quad \partial\Omega, \\ \int_\Omega h_i &=& 0, \end{array} \right. \quad \text{with} \quad \left\{ \begin{array}{rcl} -\Delta v_i &=& \delta_i \quad \text{in} \quad \Omega, \\ v_i &=& 0 \quad \text{on} \quad \partial\Omega, \end{array} \right. \tag{4.36}$$

with $\delta_i(x) := \delta(x - x_i)$. The derivations of the above formulas can be found in [33], for instance.

Now, we have all elements to apply Algorithm 1 for solving the proposed pointwise source reconstruction problem. In fact, let us consider that $\Omega = (-0.5, 0.5) \times (-0.5, 0.5)$. The target consists of three pointwise sources as shown in Fig. 7(a), where the radius of each ball represents the associated intensities. Here, we impose $U = 0$ and observe Q on $\partial\Omega$. The initial guess $b \in C_\delta(\Omega)$ is identically zero, that is $b = 0$ in Ω. The obtained result is shown in Fig. 7(b), where the locations and intensities are perfectly reconstructed.

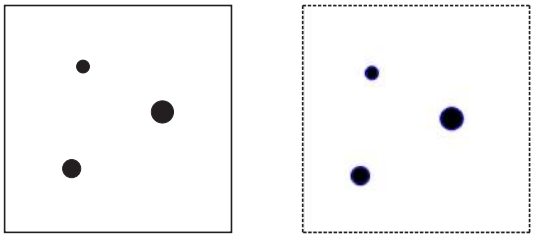

(a) target (b) result

FIGURE 7. Target and obtained result for the pointwise source reconstruction problem [33].

4.4. **Obstacles Reconstruction Problem.** Let $\mathcal{D} \subset \mathbb{R}^2$ be an open and bounded domain with smooth boundary Γ_M. We introduce a subset Ω of $\mathcal{D}$ such that $\Omega = \mathcal{D} \setminus \overline{\omega_0}$, with $\omega_0 \Subset \mathcal{D}$. The boundary of Ω is split into two disjoints parts Γ_M and Γ_0, where Γ_0 is used to denote the boundary of the hole ω_0. Let us consider the domain $\Omega^* = \Omega \setminus \overline{\omega^*}$, where $\omega^* \Subset \Omega$ represents a number $N^* \in \mathbb{N}$ of unknown holes (obstacles) within Ω^*. The boundary of Ω^* is split into three disjoints subsets Γ_M, Γ_0 and $\partial\omega^*$, where $\partial\omega^*$ is used to denote the boundaries of the N^* obstacles ω^*. See sketch in Fig. 8. The inverse problem we are dealing with consists in finding ω^* such that the following over-determined boundary value problem is satisfied:

$$\left\{\begin{array}{rcll} \Delta u^* & = & 0 & \text{in } \Omega^*, \\ u^* & = & 0 & \text{on } \Gamma_0, \\ u^* & = & 0 & \text{on } \partial\omega^*, \\ u^* & = & U & \\ -\partial_n u^* & = & Q & \text{on } \Gamma_M, \end{array}\right. \tag{4.37}$$

where U and Q are the Cauchy data on Γ_M. We assume that the flux Q is imposed while the potential U is measured.

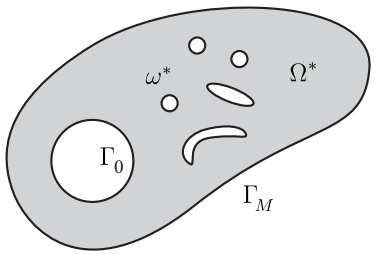

FIGURE 8. The inverse obstacles problem.

Since the inverse problem (4.37) is written in the form of an ill-posed and over-determined boundary value problem, the idea is to rewrite it as a topology optimization problem, namely

$$\underset{\Omega \subset \mathcal{D}}{\text{Minimize}} \quad \mathcal{J}_\Omega(u) = \int_{\Gamma_M} (u - U)^2. \tag{4.38}$$

Some terms in the above minimization problem require explanation. The shape functional $\mathcal{J}_\Omega(u)$ measures the misfit between the boundary measurement U and the trace on Γ_M of the solution $u = u(\Omega)$ to the following auxiliary boundary value problem depending on the boundary data Q

$$\left\{\begin{array}{rcll} \Delta u & = & 0 & \text{in } \Omega, \\ u & = & 0 & \text{on } \Gamma_0, \\ -\partial_n u & = & Q & \text{on } \Gamma_M. \end{array}\right. \tag{4.39}$$

The topological derivative concept is used for solving problem (4.38), which has been specifically designed to deal with such a topology optimization problem. In particular, the domain

Ω is perturbed by the nucleation of N ball-shaped holes of radii ε_i and centers at $x_i \in \Omega$, with $i = 1, \cdots, N$. In this case, $\alpha = \alpha(\varepsilon)$, whose entries $\alpha_i(\varepsilon_i)$ have to satisfy the constraint

$$u(x_i) - \alpha_i(\varepsilon_i)\left(\frac{1}{2\pi}\ln\varepsilon_i + g_i(x_i)\right) - \sum_{\substack{j=1\\ j\neq i}}^{N} \alpha_j(\varepsilon_j)\left(\frac{1}{2\pi}\ln\|x_i - x_j\| + g_j(x_i)\right) = 0, \tag{4.40}$$

with each g_j solution to the following auxiliary boundary value problem

$$\left\{\begin{array}{rcll} \Delta g_j &=& 0 & \text{in } \Omega, \\ \partial_n g_j &=& \partial_n \phi_j & \text{on } \Gamma_M, \\ g_j &=& \phi_j & \text{on } \Gamma_0, \end{array}\right. \tag{4.41}$$

where ϕ_j is the fundamental solution for the Laplacian into two spatial dimensions, namely

$$\phi_j(x) = \frac{1}{2\pi}\ln\|x - x_j\|, \quad \forall x \in \Omega. \tag{4.42}$$

Finally, the entries of vector $d(\xi) \in \mathbb{R}^N$ and matrix $H(\xi) \in \mathbb{R}^N \times \mathbb{R}^N$ in (3.4) are respectively defined as

$$d_i = \int_{\Gamma_M} (u - U)G_i \quad \text{and} \quad H_{ij} = \int_{\Gamma_M} G_i G_j, \tag{4.43}$$

where the auxiliaries functions G_j are solutions to

$$\left\{\begin{array}{rcll} -\Delta G_j &=& \delta_j & \text{in } \Omega, \\ \partial_n G_j &=& 0 & \text{on } \Gamma_m, \\ G_j &=& 0 & \text{on } \Gamma_0, \end{array}\right. \tag{4.44}$$

with $\delta_j := \delta(x - x_j)$ used to denote the Dirac delta distribution. The derivations of the above formulas can be found in [36], for instance.

Remark 1. *Note that $g_j(x) = g_j(x; x_j)$, because $\phi_j(x) = \phi_j(x; x_j)$ depends on the point x_j where the hole is nucleated. It means that function $g_j(x)$ depends on x_j. Therefore, the complexity order associated with the computation of all g_j may become very high. However, we will show through some numerical experiments that this term is crucial for solving the topology optimization problem* (4.38) *or equivalently the inverse problem* (4.37)*, can be seen as the main theoretical contribution from* [36].

In order to fix these ideas, let us present a simple example. We consider the domain Ω given by a circle centered at $(0, 0)$ and with unit radius. In addition, Ω has a hole ω_0 centered at $(-0.5, 0)$ and with radius 0.3. The target domain Ω^* has three hidden circular obstacles represented by black circles, as shown in Fig. 9(a). An uniform flux $Q = 1$ is applied on Γ_M, where the associated potential U is measured. The resulting reconstruction obtained from Algorithm 1 are represented by black circles as shown in Fig. 9(b).

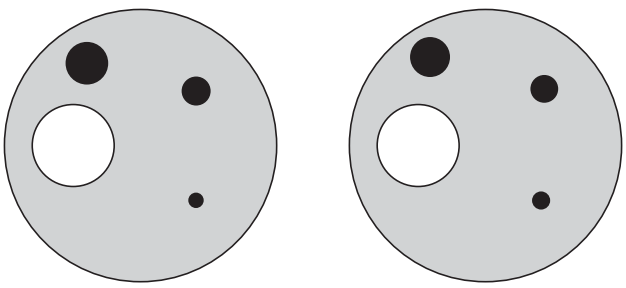

(a) target (b) result

FIGURE 9. Target and associated result for the inverse obstacle problem [36].

4.5. **Electromagnetic Casting Problem.** The inverse electromagnetic casting problem consists in looking for a suitable set of electric wires such that the electromagnetic field induced by an alternating current passing through them makes a given mass of liquid metal assumes a shape according to the electromagnetic field. An interesting and difficult problem consists in determining the topology of such inductors such that the liquid metal acquires a predefined shape. In the paper [13] a new method for the topology design of inductors in inverse electromagnetic casting problem has been proposed. See also [14]. It relies on the topological derivative concept. The basic ideas consists in write the inverse electromagnetic casting problem in the form of a topology optimization problem, where the associated shape functional is minimized with respect to a set of ball shaped inductors. Based on the obtained theoretical result, a topology design algorithm of inductors has been devised. In those papers, several numerical examples are presented showing that the proposed technique is effective to design suitable inductors.

5. Perspectives and Open Problems

In this third and last part of the series of review papers on the topological derivative concept a second order method has been presented, together with a set of applications in the context of inverse reconstruction problems. The general idea consists in rewrite the inverse problem as a topology optimization problem, where a shape functional measuring the misfit between the boundary measurements and the solution obtained from the model is expanded with respect to a set of ball-shaped anomalies. The resulting expansion is then truncated up to the second order term, leading to a quadratic and strictly convex form with respect to the parameters under consideration. Therefore, the truncated expansion has been used to devise a novel non-iterative reconstruction algorithm based on a simple optimization step. As a result, the reconstruction process becomes very robust with respect to noisy data and also independent of any initial guess. Finally, these ideas are used for solving a wide class of inverse reconstruction problems. Since the proposed method can approximate accurately the unknown set of hidden anomalies by several balls, it can be used for supplying a good initial guess for more complex iterative approaches such as the ones based on level-sets methods [32], for instance. We would like to stress however that the methodology here presented is quite recent. Therefore, it is still not clear on how to use the second order topological derivative concept. In particular, for future developments on this branch of shape-topological second order method we highlight:

(1) There is no stability and resolution analysis for the second order topological derivative based imaging functional. To demonstrate these properties in general, or at least for some particular inverse reconstruction problems, would be an important contribution to the field.
(2) Replace the Newton Method based on the second order topological derivative by a family of Quasi-Newton Methods seems to be an interesting and innovative research topic, deserving investigation.
(3) The bottleneck of the reconstruction Algorithm 1 relies on its complexity given by formula (3.6) for a high number of trial balls N, with $M \gg N$. Some insight on how to deal with such a complexity issue can be found in [33]. However, it can be seen as an interesting and still open problem.
(4) The extension of the second order topological derivative to the context of defects detection in elasticity or elastodynamics can also be investigated by using the matching asymptotic method presented in the first part of this series of review papers. However, the technical difficulties that should arise have to be considered.
(5) Applications of the second order method to other class of problems, including all those presented in the second part of this series of review papers, can also be seen as a very interesting and sometimes difficult research topic. In fact, it requires the development of new asymptotic formulas. In addition, many of these mentioned problems have no unique solution, so that the infinity dimensional Hessian matrix could degenerate. Therefore, new regularization strategies would be required to get well-posedness.

Acknowledgements

This research was partly supported by CNPq (Brazilian Research Council), CAPES (Brazilian Higher Education Staff Training Agency) and FAPERJ (Research Foundation of the State of Rio de Janeiro). These supports are gratefully acknowledged. We would also like to thanks Habib Ammari, Alfredo Canelas, Michael Hintermüller, Hyeonbae Kang, Antoine Laurain, Jairo Faria and the former students Andrey Ferreira, Thiago Machado and Suelen Rocha.

References

[1] H. Ammari, E. Bretin, J. Garnier, W. Jing, H. Kang, and A. Wahab. Localization, stability, and resolution of topological derivative based imaging functionals in elasticity. *SIAM Journal on Imaging Sciences*, 6(4):2174–2212, 2013.

[2] H. Ammari, P. Calmon, and E. Iakovleva. Direct elastic imaging of a small inclusion. *SIAM Journal on Imaging Sciences*, 1:169–187, 2008.

[3] H. Ammari and H. Kang. High-order terms in the asymptotic expansions of the steady-state voltage potentials in the presence of inhomogeneities of small diameter. *SIAM Journal on Mathematical Analysis*, 34(5):1152–1166, 2003.

[4] H. Ammari and H. Kang. *Reconstruction of small inhomogeneities from boundary measurements*. Lectures Notes in Mathematics vol. 1846. Springer-Verlag, Berlin, 2004.

[5] S. Amstutz, I. Horchani, and M. Masmoudi. Crack detection by the topological gradient method. *Control and Cybernetics*, 34(1):81–101, 2005.

[6] M. Bonnet. Higher-order topological sensitivity for 2-D potential problems. *International Journal of Solids and Structures*, 46(11–12):2275–2292, 2009.

[7] M. Bonnet and R. Cornaggia. Higher order topological derivatives for three-dimensional anisotropic elasticity. *ESAIM. Control, Optimisation and Calculus of Variations*, 2017, to appear.

[8] M. Brühl, M. Hanke, and M. S. Vogelius. A direct impedance tomography algorithm for locating small inhomogeneities. *Numerische Mathematik*, 93(4):635–654, 2003.

[9] M. Burger. A level set method for inverse problems. *Inverse Problems*, 17:1327–1356, 2001.

[10] A. P. Calderón. On an inverse boundary value problem. *Computational and Applied Mathematics*, 25(2-3):133–138, 2006. Reprinted from the Seminar on Numerical Analysis and its Applications to Continuum Physics, Sociedade Brasileira de Matemática, Rio de Janeiro, 1980.

[11] A. Canelas, A. Laurain, and A. A. Novotny. A new reconstruction method for the inverse potential problem. *Journal of Computational Physics*, 268:417–431, 2014.

[12] A. Canelas, A. Laurain, and A. A. Novotny. A new reconstruction method for the inverse source problem from partial boundary measurements. *Inverse Problems*, 31(7):075009, 2015.

[13] A. Canelas, A. A. Novotny, and J. R. Roche. A new method for inverse electromagnetic casting problems based on the topological derivative. *Journal of Computational Physics*, 230:3570–3588, 2011.

[14] A. Canelas, A. A. Novotny, and J. R. Roche. Topology design of inductors in electromagnetic casting using level-sets and second order topological derivatives. *Structural and Multidisciplinary Optimization*, 50(6):1151–1163, 2014.

[15] Y. Capdeboscq and M. S. Vogelius. A general representation formula for boundary voltage perturbations caused by internal conductivity inhomogeneities of low volume fraction. *Mathematical Modelling and Numerical Analysis*, 37(1):159–173, 2003.

[16] Y. Capdeboscq and M. S. Vogelius. Optimal asymptotic estimates for the volume of internal inhomogeneities in terms of multiple boundary measurements. *Mathematical Modelling and Numerical Analysis*, 37(2):227–240, 2003.

[17] A. Carpio and M.L. Rapún. *Topological Derivatives for Shape Reconstruction*, pages 85–133. Springer, Berlin, Heidelberg, 2008.

[18] F. Caubet, C. Conca, and M. Godoy. On the detection of several obstacles in 2D Stokes flow: Topological sensitivity and combination with shape derivatives. *Inverse Problems and Imaging*, 10(2):327–367, 2016.

[19] D. J. Cedio-Fengya, S. Moskow, and M. S. Vogelius. Identification of conductivity imperfections of small diameter by boundary measurements. Continuous dependence and computational reconstruction. *Inverse Problems*, 14(3):553–595, 1998.

[20] J. Rocha de Faria and A. A. Novotny. On the second order topologial asymptotic expansion. *Structural and Multidisciplinary Optimization*, 39(6):547–555, 2009.

[21] A.D. Ferreira and A. A. Novotny. A new non-iterative reconstruction method for the electrical impedance tomography problem. *Inverse Problems*, 33(3):035005, 2017.

[22] A. Friedman and M. Vogelius. Identification of small inhomogeneities of extreme conductivity by boundary measurements: a theorem on continuous dependence. *Archive for Rational Mechanics and Analysis*, 105(4):299–326, 1989.

[23] B. B. Guzina and M. Bonnet. Small-inclusion asymptotic of misfit functionals for inverse problems in acoustics. *Inverse Problems*, 22(5):1761–1785, 2006.

[24] M. Hintermüller and A. Laurain. Electrical impedance tomography: from topology to shape. *Control and Cybernetics*, 37(4):913–933, 2008.
[25] M. Hintermüller, A. Laurain, and A. A. Novotny. Second-order topological expansion for electrical impedance tomography. *Advances in Computational Mathematics*, 36(2):235–265, 2012.
[26] V. Isakov. *Inverse source problems*. American Mathematical Society, Providence, Rhode Island, 1990.
[27] V. Isakov. *Inverse problems for partial diferential equations*. Springer, New York, 1998.
[28] V. Isakov, S. Leung, and J. Qian. A fast local level set method for inverse gravimetry. *Communications in Computational Physics*, 10(4):1044–1070, 2011.
[29] L. Jackowska-Strumiłło, J. Sokołowski, A. Żochowski, and A. Henrot. On numerical solution of shape inverse problems. *Computational Optimization and Applications*, 23(2):231–255, 2002.
[30] R. Kohn and M. Vogelius. Determining conductivity by boundary measurements. *Comm. Pure Appl. Math.*, 37(3):289–298, 1984.
[31] A. Laurain, M. Hintermüller, M. Freiberger, and H. Scharfetter. Topological sensitivity analysis in fluorescence optical tomography. *Inverse Problems*, 29(2):025003,30, 2013.
[32] A. Leitão and J. Baumeister. *Topics in Inverse Problems*. IMPA Mathematical Publications, Rio de Janeiro, 2005.
[33] T. J. Machado, J. S. Angelo, and A. A. Novotny. A new one-shot pointwise source reconstruction method. *Mathematical Methods in the Applied Sciences*, 40(15):1367–1381, 2017.
[34] M. Masmoudi, J. Pommier, and B. Samet. The topological asymptotic expansion for the Maxwell equations and some applications. *Inverse Problems*, 21(2):547–564, 2005.
[35] A. A. Novotny and J. Sokołowski. *Topological derivatives in shape optimization*. Interaction of Mechanics and Mathematics. Springer-Verlag, Berlin, Heidelberg, 2013.
[36] S. S. Rocha and A. A. Novotny. Obstacles reconstruction from partial boundary measurements based on the topological derivative concept. *Structural and Multidisciplinary Optimization*, 55(6):2131–2141, 2017.
[37] M. Silva, M. Matalon, and D.A. Tortorelli. Higher order topological derivatives in elasticity. *International Journal of Solids and Structures*, 47(22–23):3053–3066, 2010.
[38] P. Tricarico. Global gravity inversion of bodies with arbitrary shape. *Geophysical Journal International*, 195(1):260–275, 2013.

(A.A. Novotny) Laboratório Nacional de Computação Científica LNCC/MCT, Coordenação de Matemática Aplicada e Computacional, Av. Getúlio Vargas 333, 25651-075 Petrópolis - RJ, Brasil
E-mail address: novotny@lncc.br

(J. Sokołowski) Institut Élie Cartan, UMR 7502 Laboratoire de Mathématiques, Université de Lorraine, Nancy 1, B.P. 239,54506 Vandoeuvre Lès Nancy Cedex, France
E-mail address: Jan.Sokolowski@univ-lorraine.fr

(A. Żochowski) Systems Research Institute of the Polish Academy of Sciences, ul. Newelska 6, 01-447 Warszawa, Poland
E-mail address: Antoni.Zochowski@ibspan.waw.pl